Journal of Photochemistry and Photobiology A: Chemistry 214 (2010) 115–120

Contents lists available at ScienceDirect

Journal of Photochemistry and Photobiology A: Chemistry

journal homepage: www.elsevier.com/locate/jphotochem

Excited-state absorption investigation of a cationic porphyrin derivative

R.V. Maximiano[a], E. Piovesan[b], S.C. Zílio[b], A.E.H. Machado[c], R. de Paula[d,e], J.A.S. Cavaleiro[d], I.E. Borissevitch[f], A.S. Ito[f], P.J. Gonçalves[g], N.M. Barbosa Neto[a,h,*]

[a] Instituto de Física, Universidade Federal de Uberlândia, Av. João Naves de Ávila 2121, 38400-902 Uberlândia, MG, Brazil
[b] Instituto de Física de São Carlos, Universidade de São Paulo, Caixa Postal 369, 13560-970 São Carlos, SP, Brazil
[c] Instituto de Química, Universidade Federal de Uberlândia, Av. João Naves de Ávila 2121, 38400-902 Uberlândia, MG, Brazil
[d] Universidade de Aveiro, Departamento de Química, 3810-193 Aveiro, Portugal
[e] Universidade Federal do Recôncavo da Bahia, Centro de Formação de Professores Campus Amargosa, 45.300-000 - Amargosa-BA/Brazil
[f] Faculdade de Filosofia Ciências e Letras de Ribeirão Preto, Universidade de São Paulo, Av. Bandeirantes 3900, 14040-901 Ribeirão Preto, SP, Brazil
[g] Instituto de Física, Universidade Federal de Goiás, Caixa Postal 131, 74001-970 Goiânia, GO, Brazil
[h] Departamento de Física, Universidade Federal de Minas Gerais, Caixa Postal 702, 30161-970 Belo Horizonte, MG, Brazil

ARTICLE INFO

Article history:
Received 1 March 2010
Received in revised form 1 June 2010
Accepted 7 June 2010
Available online 19 June 2010

Keywords:
Porphyrin
White-light Z-scan
Laser flash photolysis
Excited-state absorption

ABSTRACT

This work presents a complete investigation on the excited-state absorption of a new porphyrin derivative, the free-base 5,10,15,20-tetrakis (1,3-dimethylimidazolium-2-yl) porphyrin tetraiodide (H_2-TDMImP), for which the excited singlet and triplet transient absorption spectra were obtained. In order to accomplish this task, we employed the laser flash photolysis (LFP) technique in association with the white-light continuum (WLC) Z-scan measurements. The transient singlet absorption spectrum shows a reverse saturable absorption around the Q-band region (500–650 nm) and a small saturable absorption around 650 nm. From LFP experiments we verified that this porphyrin presents a biexponential decay profile, with a low quantum yield for triplet state formation. Besides, we observed that the reverse saturable absorption also takes place in triplet state.

1. Introduction

Photophysical properties of porphyrin derivatives have been the target of a huge amount of investigations during the past few decades, motivated by the possibilities of their use in a large variety of applications including light harvesting systems [1], photodynamic therapy [2], chemical sensors [3,4] and others. In general, these studies have the purpose of correlating the porphyrin molecular structure to some photophysical characteristic that can be modified upon substitution of a central ion, the attachment of outlying or axial groups, etc. It is worth to mention that in order to accomplish this task, it is imperative the development of new techniques or experimental approaches that combine different methods already existing.

Regarding to the structural aspect, porphyrins are molecules where four pyrrole rings forming a square, are connected by unsaturated methine bridges to complete a macrocycle [5,6]. In general, metalloporphyrins have the central part of the ring occupied by a metal ion linked to two pyrrole rings to yield the necessary structural stability [5–7]. Concerning to optical properties, porphyrins usually present strong absorption at the UV–Vis region, emission at the Vis–NIR region, and nonlinear optical properties that are associated to good photostability [7–10]. Theses properties are consequence of the extensively delocalized π-electron system and their planar configuration [10]. The interest in nonlinear optical processes arises mainly because the potential use of macrocycle systems as optical limiters [11,12] and switches [13], which can be achieved by sequential two photon absorption – saturable and reverse saturable absorption [14–16] – as well as simultaneous multi-photon absorption [17,18]. For this purpose, the excited-state absorption characterization is necessary for both singlet and triplet states.

In this work we employed a set of optical techniques to completely investigate the excited-state absorption from singlet and triplet states of a new cationic porphyrin derivative (the free-base 5,10,15,20-tetrakis (1,3-dimethylimidazolium-2-yl) porphyrin tetraiodide (H_2-TDMImP), with new outlying features, whose structure is shown in Scheme 1.

The singlet excited-state absorption was obtained along the Q-band, through the use of a new extension of Z-scan technique [19,20] named white-light continuum Z-scan [21,22]. We observed that for this porphyrin, the singlet state presents reverse saturable

---

* Corresponding author at: Instituto de Física, Universidade Federal de Uberlândia, Av. João Naves de Ávila 2121, 38400-902 Uberlândia, MG, Brazil. Tel.: +55 34 3239 4190; fax: +55 34 3239 4106.
E-mail address: newtonfisico@gmail.com (N.M. Barbosa Neto).

1010-6030/$ – see front matter © 2010 Elsevier B.V. All rights reserved.
doi:10.1016/j.jphotochem.2010.06.007

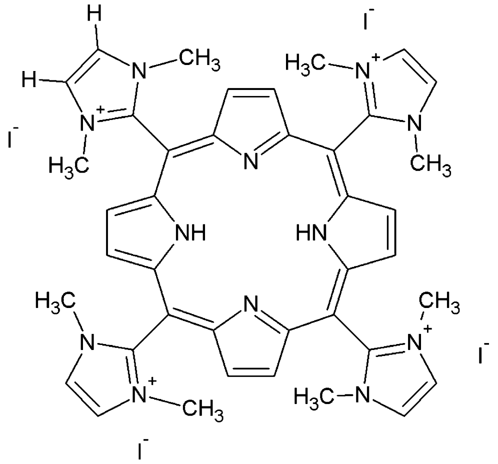

Scheme 1. Representation of the molecular structure of the free-base 5,10,15,20-tetrakis (1,3-dimethylimidazolium-2-yl) porphyrin tetraiodide (H_2-TDMImP).

absorption (RSA) at the Q-band region and a small saturable absorption (SA) close to 655 nm. The transient absorption triplet spectra (TA) were obtained using laser flash photolysis (LFP) technique that also allows of the obtaining the quantum efficiency for triplet formation and its decay time. We observed a triplet decay time around 2 μs, and low quantum efficiency of triplet formation (∼8%). Moreover, LFP data also show that the studied porphyrin presents a negative transient absorption between 450 nm up to 540 nm, which suggests an increase in the absorbance as compared to the singlet ground-state absorption. Such increase in the absorbance points to a reverse saturable absorption, where the excited-state absorption cross-section is greater than the ground-state absorption cross-section. Besides the RSA, a small saturable absorption (SA), the reciprocal process of RSA, around 545 nm is observed for excited triplet states. Above 550 nm, no transient absorption signal is observed.

2. Experimental section

The synthesis of the new porphyrins derivative studied herein was carried out under Adler-Longo conditions [23] and is detailed reported in Ref. [24].

All photophysical measurements were performed in aqueous solution under room temperature, with samples placed in a 1 cm optical path quartz cuvette. The UV–Vis absorption spectra were acquired in a Shimadzu UV-250 1 PC spectrophotometer and the fluorescence spectra were acquired exciting the sample with a Xenon lamp and detecting the signal in a USB 2000 Ocean Optics spectrophotometer in right angle configuration. Before hit the sample, the excitation light was passed through a monochromator in order to select the appropriate pumping wavelength. Fluorescence lifetime measurements were performed in an apparatus based on the time correlated single photon counting method. The excitation source was a titanium–sapphire laser, whose frequency was doubled to 465 nm in a LBO crystal, pumped by the second harmonic of a diode-pumped Nd:YVO_4 laser. The signal was detected next the fluorescence maximum at 640 nm. The singlet excited-state absorption was obtained with the white-light continuum Z-scan technique [21,22], which employs a conventional Z-scan [19,20] experimental setup but uses a broadband coherent light as pump source. The WLC is focused, using an achromatic lens, onto the nonlinear sample that is scanned along the z-direction, and the transmitted beam is totally focused into a portable spectrometer. WLC from 450 to 700 nm was produced by focusing 150 fs laser pulses at 775 nm, generated by a 1 kHz commercial Ti:sapphire chirped pulse amplified system, with $f = 11$ cm lens into a 4 cm-thick cell containing distilled water. The pump power control was performed with calibrated neutral density filters. The energy at a specific wavelength of the WLC was determined by considering the continuum as formed by a group of nearly bandwidth-limited pulses centered at various wavelengths. Using the spectral distribution and the WLC total energy, the energy of each small bandwidth can be estimated. The chirp rate of the WLC pulse (18 fs/nm) was determined trough optical Kerr effect measurements [21,25,26] in hexane [25,26], using a strong pump pulse at 775 nm and the weaker WLC beam as probe. Owing to the group velocity dispersion, the bluer intrapulse components are approximately 4 ps delayed in respect to those in the red. This procedure was performed in a theoretical fitting, in order to compensate possible accumulative contributions from excited-state absorption [27,28]. In the Z-scan experiments the sample was placed in a 0.2 cm optical cell in order to assure the thin sample approximation. For more details of WLC Z-scan experimental setup see Ref. [21,22]. Laser flash photolysis (LFP) experiments were carried out by producing excited states with 3 ns laser pulses at 532 nm, delivered by frequency doubled Q-switched Nd:YAG laser. Decay profiles of the triplet state absorption were measured probing the sample with a Xenon lamp and detecting the signal with a photomultiplier tube connected to a 600 MHz digital oscilloscope. In the LFP technique we are able to measure the transient absorption spectrum exciting the sample with the nanosecond pulse laser and probing it with the appropriated wavelength selected from the emission of a continuum Xenon lamp with the use of a monochromator. Aiming to avoid cumulative effects in the LFP measurements the excited state was generated with 3 ns single shot pulses and the average transient absorption were obtained from 64 shots for each decay profile. In order to verify the influence of the O_2 on the triplet decay time gaseous nitrogen was injected for 10 min into the solution containing the compound. The LFP decay profile of this solution was compared to the obtained for the solution without nitrogen injection.

To guarantee that no photochemical reaction takes place during LFP measurements, the complete UV–Vis porphyrin absorption spectrum was monitored before and after the measurements with pulsed laser. No modifications in the monitored spectra were observed, indicating that the sample is photostable.

3. Results and discussions

Energy gaps between the energy levels, obtained by previous TD-DFT calculations [24], suggests that light-matter interaction processes for these porphyrins occurs, at UV–Vis region, according the Jablonski diagram depicted in Fig. 1. This diagram is formed by five-energy level that considers the ground-state singlet level (S_0), excited singlet (S_1 and S_2) and triplet levels (T_1 and T_2) with possible up and down-ward (radiative and non-radiative) and intersystem crossing transitions among them [7,29].

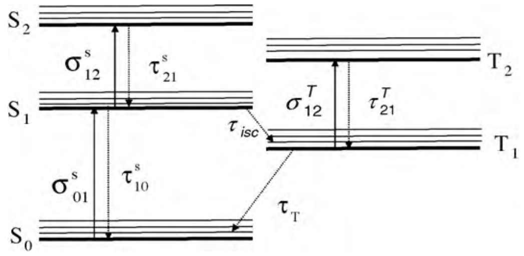

Fig. 1. Jablonski diagram used to describe the typical photophysical behavior in free-base porphyrin derivatives.

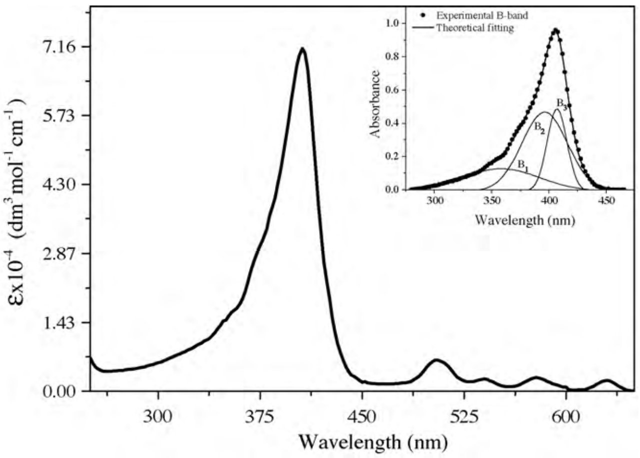

Fig. 2. UV–Vis absorption spectrum of H_2-TDMImP in aqueous solution. The inset shows the deconvolution of the Soret band with B_1, B_2 and B_3 sub-bands.

The acronyms S_1 and S_2 were used to designate the excited states immediately superior to the ground state. Data from TD-DFT calculation suggest that these electronic states are related to complex sets of electronic, giving to these states a multiconfigurational character [24].

3.1. Ground state

The UV–Vis absorption spectrum of H_2-TDMImP in aqueous solution is shown in Fig. 2. It presents a strong B or Soret band with maximum wavelength around 406 nm, assigned to the $S_0 \rightarrow S_2$ transition, and Q-bands located between 479 nm and 650 nm, related to the $S_0 \rightarrow S_1$ transition.

Gaussian deconvolution of the Soret band (see inset of Fig. 2) suggests that it is constituted by three overlapping sub-bands, related to B band vibrational modes. The first one is responsible for the small shoulder around 357 nm (B_1), [30] the second is located around 396 nm (B_2). The third one, located around 407 nm (B_3), is the strongest of them. The main peak is formed by a combination of the B_2 and B_3 vibrational modes, while B_1 is responsible mainly by the broadening of the Soret band, having smaller amplitude. Table 1 summarizes the features of the Soret band in H_2-TDMImP porphyrin.

Concerning to the Q-band, the number of Q-bands depends on the symmetry of the molecule. For symmetrical metalloporphyrins, of D_{4h} symmetry, the number of peaks is two. One of them, Q(0,0), is related to the lowest excited singlet state, while the other, Q(1,0), is the next vibrational excitation of the lowest excited singlet state. The equivalent free-base porphyrins, with two hydrogen atoms at the inner part of the porphyrin ring have the symmetry reduced from D_{4h} to D_{2h}. As consequence, there is an increase from 2 to 4 Q-bands. The degeneracy of the vibrational modes is broken, thus splitting Q(0,0) into Q_x(0,0) and Q_y(0,0) and Q(1,0) into Q_x(1,0) and Q_y(1,0).

In order to obtain the relative strength of Q-band absorption we followed Spellane et al. [29], and use Eq. (1) to calculate the Q(0,0)/Q(1,0) absorbance ratio:

$$\frac{Q(0,0)}{Q(1,0)} = \left[\frac{Q_x(0,0)+Q_y(0,0)}{Q_x(1,0)+Q_y(1,0)}\right] \qquad (1)$$

obtaining a value equal to 0.45, which is in the same order of magnitude of other free-base porphyrins [30,31]. Other Q absorbance band features are summarized in Table 2 Table 2.

Table 1
Soret band spectroscopic characteristics. λ_c is position of the maximum, $\Delta\lambda$ is the bandwidth (FWHM) and A_i/A_3 is the relative amplitude related to the most intense sub-band B_3.

Soret band	λ_c (nm)	$\Delta\lambda$ (nm)	(A_i/A_3)
B_1	376	42	0.43
B_2	398	20	0.73
B_3	409	16	1

Table 2
Q-band spectroscopic characteristics. λ_c is position of the maximum of the band and $\Delta\lambda$ is the bandwidth (FWHM).

Q-band	λ_c (nm)	$\Delta\lambda$ (nm)
Q_y(1,0)	505	18
Q_y(0,0)	540	11
Q_x(1,0)	578	22
Q_x(0,0)	629	16

3.2. Singlet excited state

Fig. 3 presents the fluorescence spectrum of porphyrin in aqueous solution when excited at the B band region (400 nm). There are clearly three emission bands located at 596 nm, 638 nm and 704 nm.

The sample excitation at the B band results in a small Stokes shift (around 8 nm) of the peaks at 638 nm and 704 nm, related to end of the Q-band. Since the sample was pumped at the B band we conclude that the molecule first relax to the lowest vibronic state of the Q-band ($\nu = 0$) before decay to the ground state, emitting the observed fluorescence associated to $0 \rightarrow 0$ and $0 \rightarrow 1$ transitions, a dynamics very well clarified in Ref. [30]. However, exciting the sample with different wavelengths, along the absorbance spectrum, and acquiring the ratio between the bands located at 596 nm and 638 nm, we conclude that the band centered at 596 nm is related to Q_y band, which similar to Q_x can be populated by direct $S_0 \rightarrow S_1$ excitation or by Soret band relaxation. Fluorescence emission coming from transitions of more energetic states than Q_x were previously reported for Soret Band [34,35], also presenting a very small Stokes shift.

Fig. 4 shows that the fluorescence evolution of the investigated porphyrin clearly follows a mono-exponential behavior whose fitting provide a value of 15 (±0.2) ns for the relaxation time. Although slower, this fluorescence lifetime is of the same order of magnitude of the data reported in literature [30,36,37] for other free-base porphyrins.

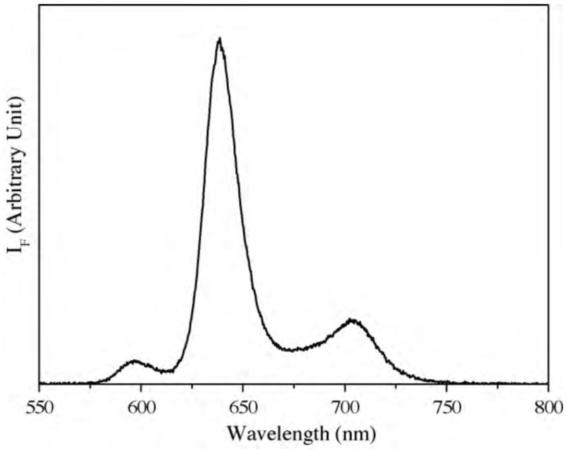

Fig. 3. Fluorescence spectra for H_2-TDMImP porphyrin in aqueous solution. λ_{exc} = 400 nm.

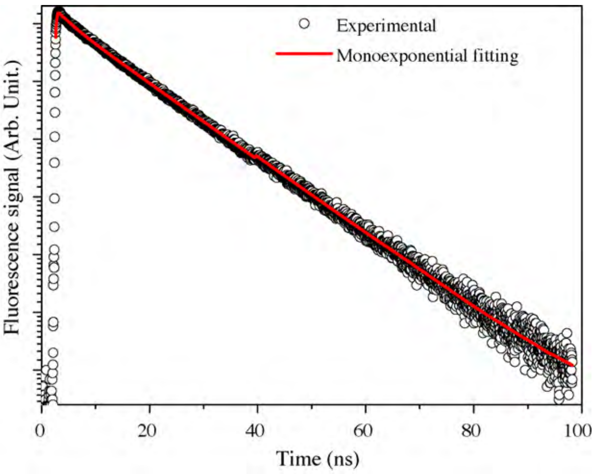

Fig. 4. Logarithm of the fluorescence decay time for the free-base porphyrin. The red continuous curves is the mono-exponential fitting.

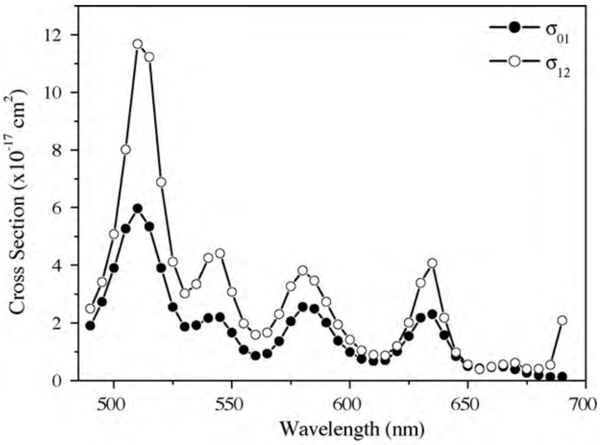

Fig. 6. Ground state (closed circles) and first singlet excited-state (open circles) absorption cross-section spectra.

In order to investigate the singlet excited-state absorption ($S_1 \rightarrow S_n$ transition), we employed the WLC Z-scan technique, which provides Z-scan signatures for each wavelength of the complete WLC range, captured simultaneously. Fig. 5 shows the normalized transmittance spectrum of H_2-TDMImP acquired with the WLC Z-scan.

A reverse saturable absorption (RSA) was detected in the blue region of the spectrum (below 500 nm) and between 507 nm and 640 nm, indicated by normalized transmittance values lower than one. A small saturable absorption (SA) was detected around 655 nm. Since the employed broadband source is resonant with the Q-band, the WLC pulse excites the porphyrin molecules to S_1. As the intersystem crossing time for free-base porphyrins is in the nanosecond scale [31–33], therefore much longer than the WLC pulse duration, the triplet states were not taken into account in the analysis. In this way, we need to consider just the three energy-level system corresponding to the left part of the Jablonski diagram (Fig. 1) in order to describe the population dynamics. Molecules excited to the first excited state can decay to S_0 with a relaxation time τ_{10}, which is also much longer than the WLC pulse duration. Moreover, the upper level, is assumed to be too short-lived to present any appreciable population build up. Consequently, molecules are accumulated in the first excited state and the absorption cross-section between these states can be determined. It is worth to mention that although the absorption of higher excited states could take place, its contribution was not observed through the modification of Z-scan signature at the focal region. Besides, the contribution of the highest excited states could be considered as a contribution for the first excited state, once we are not able to discriminate the two processes and consequently do not change the excited-state absorption dispersion. So, according to the simplified energy diagram, the rate equation used to describe the change of absorption is:

$$\frac{dn_{S_0}(t)}{dt} = -n_{S_0}(t)W^{\mathrm{up}}(\lambda) + \frac{1 - n_{S_0}(t)}{\tau_{10}} \tag{2}$$

in which $W_{01}^{\mathrm{up}}(\lambda) = \sigma_{01}(\lambda)I/h\nu$ is the upward transition rate, $\sigma_{01}(\lambda)$ is the ground-state absorption cross-section, cm^2, for a given wavelength, I is the irradiance in W/cm^2 and $n_i(t)$ are the dimensionless population fractions in the respective levels, following the closure condition: $n_{S_0}(t) + n_{S_1}(t) = 1$. The population fractions, in each level (S_0 and S_1), are determined by the rate Eq. (2), as the sample interacts with the laser pulse. So for each small time interval, along the pulse with temporal Gaussian profile, a new population is obtained and feed the Eq. (3). Such procedure allows us to obtain the change of the absorption coefficient of the sample caused by the interaction with the laser pulse. The absorption coefficient is written as:

$$\alpha(\lambda, t) = N[n_{S_0}(t)\sigma_{01}(\lambda) + n_{S_1}(t)\sigma_{12}(\lambda)] \tag{3}$$

with N being the molecular concentration and $\sigma_{12}(\lambda)$ the singlet excited-state absorption cross-section. The ground-state absorption cross-section is obtained from the linear absorbance spectra and then, the only parameter used for the fitting of the Z-scan data is the singlet excited-state absorption cross-section. It is significant to mention that any contribution of cumulative processes, caused by the white-light pulse chirp, is taken into account in the fitting procedure, considering the time dependence of the white-light components [27,28]. Fig. 6 depicts the singlet excited-state absorption cross-section together with the ground-state cross-section, indicating that they have similar shapes at the Q-band region. As previously reported [27], this is a typical behavior for porphyrins with D_{2h} symmetry, like the free bases, and indicates that the porphyrin vibronic structure remains practically unchanged upon excitation. Such result is supported by the small Stokes shift presented by the fluorescence emission. Finally, no simultaneous two-photon absorption was observed at the non-resonant region above 650 nm.

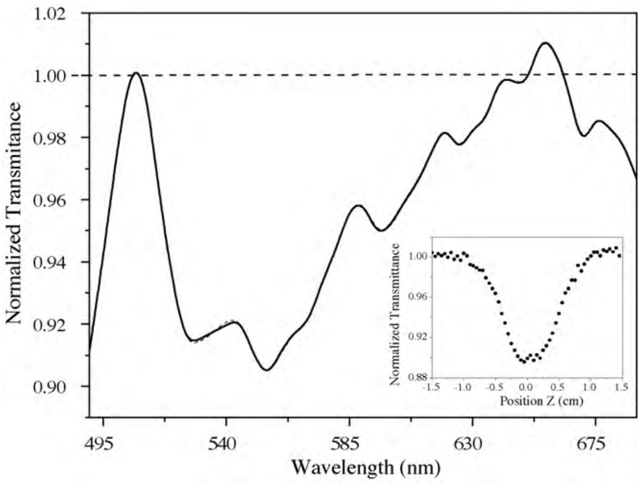

Fig. 5. Normalized transmittance spectrum for H_2-TDMImP in aqueous solution obtained with the WLC Z-scan. The inset shows a typical Z-scan RSA signature acquired for 555 nm.

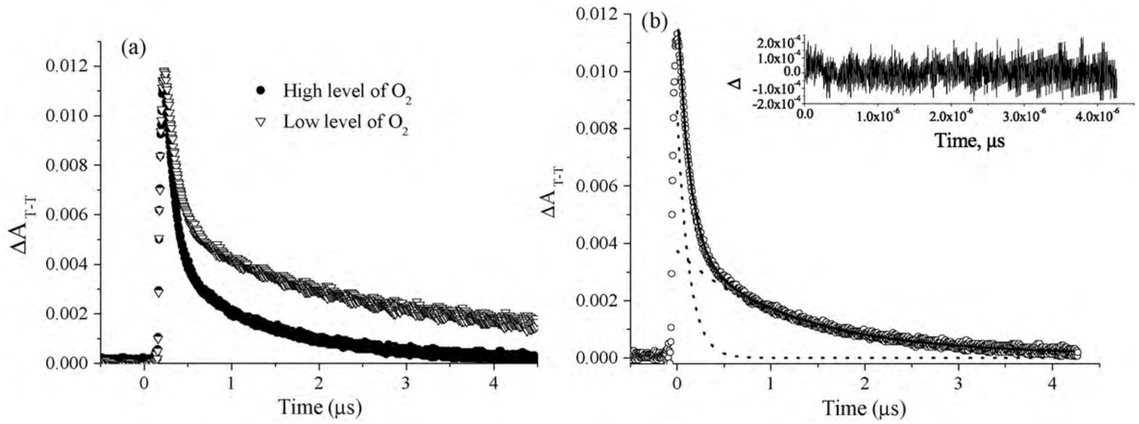

Fig. 7. (a) LFP decay curve for H_2-TDMImP obtained under high (closed circles) and low (open triangles) levels of oxygen concentration. (b) The bi- (solid line) and the mono-exponential components (dotted lines) for the decay obtained with high level of oxygen. The inset shows the residue curve. The excitation and probing wavelengths were respectively 532 nm and 470 nm. The time constants obtained were $>1 \times 10^7\ s^{-1}$ for fast component and $5 \times 10^5\ s^{-1}$ for slower one.

3.3. *Triplet excited state*

In order to investigate the triplet transient absorption spectra, lifetime and quantum yield of triplet formation, we employed LFP technique.

Fig. 7a presents curves achieved at different levels of molecular oxygen presence. The curves were just adjusted with a biexponential decay, with a fast (<100 ns) and a slow (~2 μs) components. It is worth to note that the temporal resolution of the LFP system is around 100 ns, which imply that the fast component could be yet faster. The two mono-exponential components are shown in Fig. 7b, for sample with high level of dissolved oxygen. The partial removal of the dissolved oxygen increases the contribution of the decay time related to the slow component, as can be see from Fig. 7a, which suggests that it can be associated to the decay time (τ_T) from the first excited triplet to the ground singlet state ($T_1 \rightarrow S_0$). The value measured for τ_T is small when compared to the ones estimated for other porphyrins such as the free-base tetramethyl porphyrin (H_2TMPP) [38] in the presence of O_2. Besides, the remotion of oxygen decreases the contribution of the fast component from 12% to 9%, indicating that the porphyrin-oxygen interaction is related to fast process. Moreover, such so fast decay indicates that it can be probably attributed to an excited singlet state process, for instance, excited sates absorption.

The triplet state transient absorption spectra (TA) are shown in Fig. 8 for the slow and fast decay components.

For photostable molecules, the TA measures the absorption difference between the triplet excited-state (related to $T_1 \rightarrow T_2$ transition) and the singlet ground state. In our analysis, negative values in the TA spectrum imply that the triplet excited-state absorption is stronger than the ground-state and so RSA takes place. On the other hand, a bleaching (positive values) corresponds to a SA.

The analysis of the slow relaxation associated to triplet-triplet absorption indicates that the molecule presents a RSA process at the blue part of the spectrum, followed by a small photo-bleaching between 530 nm and 560 nm. No TA signal is observed above 560 nm for the slow component, meaning that the triplet state absorption cross-section has a value close to that of the ground-state. This is also observed around 530 nm (inversion point from RSA to SA). The fast relaxation presents a similar behavior up to 550 nm, but a large increase is observed beyond. This enhancement may be attributed to contributions coming from the spontaneous emission, since it increases in the same spectral region where the porphyrin fluorescence is located. Moreover, such so fast decay, compared with the resolution of the LFP technique (100 ns), can easily enhances the magnitude of the signal without changes the transient decay curve, as we have observed.

LFP also provides the quantum yield for the triplet formation (Φ_T), which is achieved through the use of a reference molecule with a known Φ_T. To accomplish this task, we measured the TA signal of our sample and that of the free-base tetramethyl porphyrin, used as reference ($\Phi_T = 0.43$, $ABS_{532\,nm} = 0.27$) [38] and applied the Eq. (4):

$$\Phi_T^S = \Phi_T^R \frac{\Delta OD_S}{\Delta OD_R} \frac{ABS_R}{ABS_S} \tag{4}$$

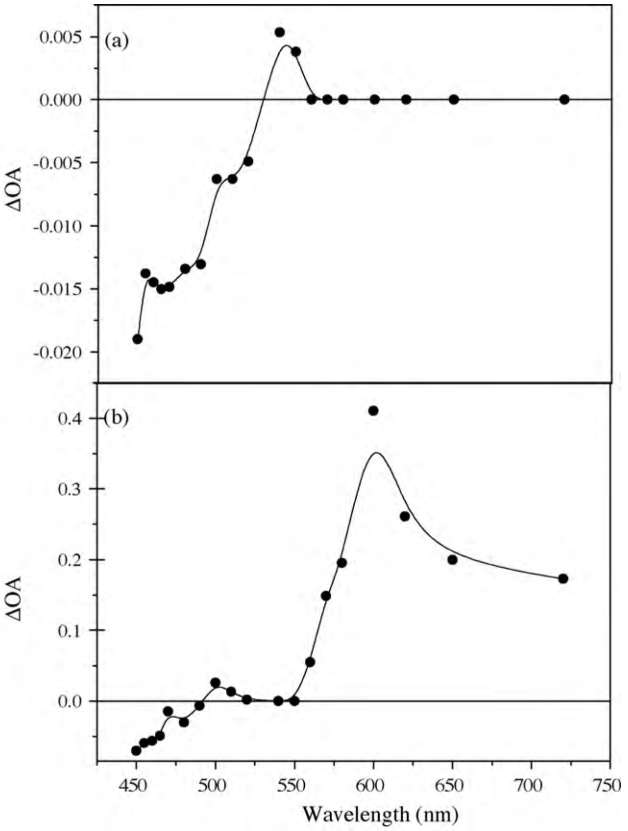

Fig. 8. Transient absorption spectra of H_2-TDMImP: (a) slow and (b) fast decay component. The solid lines are just guide for the eyes.

in which ABS means linear absorbance, S stands for sample and R for reference. We have obtained $\Phi_T = 0.08$. The intersystem crossing time can be obtained from $\Phi_T = \tau_F/\tau_{isc}$. Performing the calculations we obtain τ_{isc} near 187 ns. These results in association with the extremely low fluorescence quantum yield ($\Phi_F = 0.0004$) [24], suggests that H_2-TDMImP should decay mainly through an internal conversion process, yielding a very low triplet state population. In fact, the results indicates that the internal conversion rate is around 12 times higher than the intersystem crossing rate and two thousands higher than radiative decay rate. Such fact can be attributed to the presence of iodide ions at the outlying of the ring.

4. Conclusions

Summarizing, we have shown that H_2-TDMImP presents a RSA process in both singlet and triplet excited states, which is interesting for optical limiting applications at nano- and sub-nanosecond regimes. Besides, no two-photon absorption was observed even at the region near the absorption band (one-photon enhancement), indicating that the observed nonlinear process can be attributed to the population of the excited-state. Moreover, the sample has a very high internal conversion rate with the first singlet excited-state presenting a fluorescence lifetime of 15 ns. Such high non-radiative decay is probably caused by the iodide ions at the outlying region of the ring. The triplet state presents biexponential decay with fast and slow relaxations, being the slow process attributed to the triplet relaxation to the ground state, while the fast, although not clarified, shows to be dependent on the porphyrin-oxygen interaction. Finally, we demonstrated that the experimental approach combining Laser Flash Photolysis with the new white-light continuum Z-scan technique is extremely efficient in order to fully characterize the excited-state of chemical species at the visible region.

Acknowledgments

The authors are grateful to CNPq, INCT/INFo, FAPEMIG, CAPES and FAPESP for providing financial support to this research. Particularly, N.M. Barbosa Neto and R.V. Maximiano thanks CAPES/PROCAD project (under contract number 185/2007) for the financial support. The authors are also very thankful to the referee comments that improved considerably the quality of the manuscript. This work was funded by BZG.

References

[1] D. Gust, T.A. Moore, A.L. Moore, Mimicking photosynthetic solar energy transduction, Acc. Chem. Res. 34 (2001) 40–48.
[2] M. Ochsner, Photophysical and photobiological processes in the photodynamic therapy of tumours, J. Photochem. Photobiol. B 39 (1997) 1–18.
[3] J.H. Chou, M.E. Kosal, H.S. Nalwa, N.A. Rakow, K.S. Suslick, Applications of porphyrins and metalloporphyrins to materials chemistry, in: K. Kadish, K. Smith, R. Guillard (Eds.), The Porphyrin Handbook, Academic Press, New York, 2000, pp. 43–141.
[4] F.J. Pavinatto, A.F. Gameiro Jr., A.A. Hidalgo, L.R. Dinelli, L.L. Romualdo, A.A. Batista, N.M. Barbosa Neto, M. Ferreira, O.N. Oliveira Jr., Langmuir and Langmuir–Blodgett (LB) films of tetrapyridyl metalloporphyrins, Appl. Surf. Sci. 254 (2008) 5946–5952.
[5] M. Gouterman, Spectra of porphyrins, J. Mol. Spectrosc. 6 (1961) 138–163.
[6] M. Gouterman, G.H. Wagniére, L.C. Snyder, Spectra of porphyrins part II. The four orbital model, J. Mol. Spectrosc. 11 (1963) 108–127.
[7] K. Kalyanasundaram, Photochemistry of Polypyridine and Porphyrin Complexes, Academic Press, San Diego, 1992.
[8] K. Kandasamy, K.D. Rao, R. Deshpande, P.N. Puntambekar, B.P. Singh, S.J. Shetty, T.S. Srivastava, Z-scan studies on porphyrins derivative, Appl. Phys. B 64 (1997) 479–484.
[9] K.S. Suslick, C.-T. Chen, G.R. Meredith, L.-T. Cheng, Push–pull porphyrins as nonlinear optical materials, J. Am. Chem. Soc. 114 (1992) 6928–6930.
[10] M.O. Senge, M. Fazekas, E.G.A. Notaras, W.J. Blau, M. Zawadska, O.B. Locos, E.M.N. Mhuircheartaigh, Nonlinear optical properties of porphyrins, Adv. Mater. 19 (2007) 2737–2774.
[11] N.M. Barbosa Neto, S.L. Oliveira, L. Misoguti, C.R. Mendonça, P.J. Gonçalves, I.E. Borissevitch, L.R. Dinelli, L.L. Romualdo, A.A. Batista, S.C. Zílio, Singlet excited state absorption of porphyrin molecules for pico- and femtosecond optical limiting application, J. Appl. Phys. 99 (2006), 123103-1–123103-4.
[12] M. Calvete, G.Y. Yang, M. Hanack, Porphyrins and phthalocyanines as materials for optical limiting, Synth. Met. 141 (2004) 231–243.
[13] C. Loppacher, M. Guggisberg, O. Pfeiffer, E. Meyer, M. Bammerlin, R. Lüthi, R. Schlittler, J.K. Gimzewski, H. Tang, C. Joachim, Direct determination of the energy required to operate a single molecule switch, Phys. Rev. Lett. 90 (2003), 066107-1–166107-3.
[14] E.W. Van Stryland, D.J. Hagan, T. Xia, A.A. Said, Applications of nonlinear optics to passive optical limiters, in: H.S. Nalwa, S. Miyta (Eds.), Nonlinear Optics of Organic Molecules and Polymers, CRC Press, Boca Raton, 1997, pp. 841–860.
[15] C. Li, L. Zhang, M. Yang, H. Wang, Y. Wang, Dynamic and Steady state behavior of reverse saturable absorption in metallophtalocyanine, Phys. Rev. A 49 (1994) 1149–1157.
[16] D.S. Corrêa, L. De Boni, D.S. dos Santos Jr., N.M. Barbosa Neto, O.N. Oliveira Jr., L. Misoguti, S.C. Zílio, C.R. Mendonça, Reverse saturable absorption in chlorophyll A solutions, Appl. Phys. B 74 (2002) 559–561.
[17] A.A. Andrade, N.M. Barbosa Neto, L. Misoguti, L. De Boni, S.C. Zílio, C.R. Mendonça, Two-photon absorption investigation in reduced and oxidized cytochrome c solutions, Chem. Phys. Lett. 390 (2004) 506–510.
[18] D.S. Corrêa, L. De Boni, D.T. Balogh, C.R. Mendonça, Three- and four-photon excitation of poly(2-methoxy-5-(2′-ethylhexyloxy)-1,4-phenylenevinylene) (MEH-PPV), Adv. Mater. 19 (2007) 2653–2656.
[19] M. Sheik-Bahae, A.A. Said, E.W. Van Stryland, High-sensitivity, single-beam n_2 measurements, Opt. Lett. 17 (1989) 955–957.
[20] M. Sheik-Bahae, A.A. Said, T.-H. Wei, D.J. Hagan, E.W. Van Stryland, Sensitive measurement of optical nonlinearities using a single beam, IEEE J. Quantum Electron. 26 (1990) 760–769.
[21] L. De Boni, A.A. Andrade, L. Misoguti, C.R. Mendonça, S.C. Zílio, Z-scan measurements using femtosecond continuum generation, Opt. Express 12 (2004) 3921–3927.
[22] M. Balu, J. Hales, D.J. Hagan, E.W. Van Stryland, White-light continuum Z-scan technique for nonlinear materials characterization, Opt. Express 12 (2004) 3820–3826.
[23] D.H. Tjahjono, T. Akutsu, N. Yoshioka, H. Inoue, Cationic porphyrins bearing diazolium rings: synthesis and their interaction with calf thymus DNA, Biochim. Biophys. Acta: Gen. Subj. 1472 (1999) 333–343.
[24] A.E.H. Machado, N.M. Barbosa Neto, W.R. Gomes, D.M.S. Araújo, H.S. Miglio, L. T. Ueno, P. L. Franzen, S. C. Zilio, R. de Paula, J.A.S. Cavaleiro, Synthesis and optical characterization of two tetrasubstituted cationic porphyrin derivatives. Paper submitted to be considered for publication at Journal of Photochemistry and Photobiology A: Chemistry.
[25] R. Boyd, Nonlinear Optics, Academic Press, San Diego, 1992.
[26] A. Scodinu, J.T. Fourkas, Synthesis and optical characterization of two tetrasubstituted cationic porphyrin derivatives, J. Phys. Chem. B 107 (2003) 44–51.
[27] P.J. Gonçalves, I.E. Borissevitch, S.C. Zilio, Effect of protonation on the singlet-singlet excited-state absorption of meso-tetrakis(p-sulphonatophenyl) porphyrin, Chem. Phys. Lett. 469 (2009) 270–273.
[28] L. De Boni, L. Gaffo, L. Misoguti, C.R. Mendonça, Nonlinear absorption spectrum of ytterbium bis-phthalocyanine solution by White-light continuum Z-scan technique, Chem. Phys. Lett. 419 (2006) 417–420.
[29] J.R. Lakowicz, Principles of Fluorescence Spectroscopy, Kluwer Academic/Plenum Publishers, New York, 1999.
[30] J. Spencer, H.-Z. Yu, A.H. Zewail, Ultrafast dynamics of porphyrins in the condensed phase: I. Free base tetraphenylporphyrin, J. Phys Chem. A 106 (2002) 9837–9844.
[31] P.J. Spellane, M. Gouterman, A. Antipas, S. Kim, Y.C. Liu, Porphyrins.40. Electronic-spectra and 4-orbital energies of frees-base, zinc, copper, and palladium tetrakis(perfluorophenyl) porphyrins, Inorg. Chem. 19 (1980) 386–391.
[32] X.Z. He, G.M. Xia, Y.L. Zhou, M.H. Zhang, T. Shen, Comparative study of photophysical properties of isomeric tetrapyridyl- and tetra-(N-hexadecylpyridiniumyl) porphyrin, Spectrochim. Acta A 55 (1999) 873–880.
[33] K. Kalyanasundaram, Photochemistry of water-soluble porphyrins: comparative study of isomeric tetrapyridyl- and tetrakis(N-methylpyridiniumyl) porphyrins, Inorg. Chem. 23 (1984) 2453–2459.
[34] X. Liu, E.K.L. Yeow, S. Velate, R.P. Steer, Photophysics and spectroscopy of the higher electronic states of zinc metalloporphyrins: a theoretical and experimental study, Phys. Chem. Chem. Phys. 8 (2006) 1298–1309.
[35] H.-Z. Yu, J.S. Baskin, A.H. Zewail, Ultrafast dynamics of porphyrins in the condensed phase: II. Zinc tetraphenylporphyrin, J. Phys. Chem. A 106 (2002) 9845–9854.
[36] N.M. Barbosa Neto, L. De Boni, J.J. Rodrigues Jr., L. Misoguti, C.R. Mendonça, L.R. Dinelli, A.A. Batista, S.C. Zílio, Dynamic saturable optical nonlinearities in free base tetrapyridylporphyrin, J. Porphyr. Phthalocya. 7 (2003) 452–456.
[37] P.J. Gonçalves, L. De Boni, N.M. Barbosa Neto, J.J. Rodrigues Jr., S.C. Zílio, I.E. Borissevitch, Effect of protonation on the photophysical properties of meso-tetra(sulfonatophenyl) porphyrin, Chem. Phys. Lett. 407 (2005) 236–241.
[38] P.J. Gonçalves, L.P.F. Aggarwal, C.A. Marquezin, A.S. Ito, L. De Boni, N.M. Barbosa Neto, J.J. Rodrigues Jr., S.C. Zílio, I.E. Borissevitch, Effects of interaction with CTAB micelles on photophysical characteristics of meso-tetrakis(sulfonatophenyl) porphyrin, J. Photochem. Photobiol. A 181 (2006) 378–384.